J. Hydrol. Hydromech., 67, 2019, 1, 4–19
DOI: 10.2478/johh-2018-0013

An EnKF-based scheme for snow multivariable data assimilation at an Alpine site

Gaia Piazzi[1*], Lorenzo Campo[1], Simone Gabellani[1], Fabio Castelli[2], Edoardo Cremonese[3], Umberto Morra di Cella[3], Hervé Stevenin[4], Sara Maria Ratto[4]

[1] CIMA Research Foundation, via Armando Magliotto, 2 - 17100 Savona, Italy.
[2] Department of Civil and Environmental Engineering, University of Florence, Via Santa Marta, 350139 Florence, Italy.
[3] Environmental Protection Agency of Aosta Valley, Loc. Grande Charrière, 44 11020 Saint-Christophe, Aosta, Italy.
[4] Regional Center of Civil Protection, Aosta Valley Region, via Promis, 2/A - 11100 Aosta, Italy.
[*] Corresponding author. Tel.: +39 019230271. Fax: +39 01923027240. E-mail: gaia.piazzi@cimafoundation.org

Abstract: The knowledge of snowpack dynamics is of critical importance to several real-time applications especially in mountain basins, such as agricultural production, water resource management, flood prevention, hydropower generation. Since simulations are affected by model biases and forcing data uncertainty, an increasing interest focuses on the assimilation of snow-related observations with the purpose of enhancing predictions on snowpack state. The study aims at investigating the effectiveness of snow multivariable data assimilation (DA) at an Alpine site. The system consists of a snow energy-balance model strengthened by a multivariable DA system. An Ensemble Kalman Filter (EnKF) scheme allows assimilating ground-based and remotely sensed snow observations in order to improve the model simulations. This research aims to investigate and discuss: (1) the limitations and constraints in implementing a multivariate EnKF scheme in the framework of snow modelling, and (2) its performance in consistently updating the snowpack state. The performance of the multivariable DA is shown for the study case of Torgnon station (Aosta Valley, Italy) in the period June 2012 – December 2013. The results of several experiments are discussed with the aim of analyzing system sensitivity to the DA frequency, the ensemble size, and the impact of assimilating different observations.

Keywords: Snow modeling; Energy-balance model; Data Assimilation; Ensemble Kalman Filter.

INTRODUCTION

The seasonal presence of snow strongly impacts both the energy balance and water resource budget, not only locally, but also at larger scale. Because of its low thermal conductivity, the snowpack produces an insulating effect over the underlying soil, whose temperature variability is severely reduced towards a stable condition (Zhang, 2005). Moreover, its high albedo entails a remarkable reduction of shortwave radiation absorption, with a resulting lowering of near surface air temperature.

Snow dynamics strongly impact hydrological processes. During the winter season the presence of snow cover reduces the effective drainage. Thus, in case of possible rainfall events the watershed time of concentration turns out to be lower than in snowless condition. Moreover, the release of the significant water volume stored in winter period considerably contributes to the total discharge during the melting period (Barnett et al., 2005; Clark and Hay, 2004; Zappa et al., 2003). Melt water supplies a significant component of the annual water budget, both in terms of soil moisture and runoff, which plays a critical role in floods generation in snow-dominated basins. Therefore, when modeling hydrological processes in snow-dominated catchments the quality of predictions deeply depends on how the model succeeds in catching snow dynamics (Wood et al., 2016).

A growing effort is aimed at enhancing the physical representation of the snowpack in hydrologic models. Despite progressive improvements, several flaws endure mainly due to uncertainty in parameterizations, errors affecting both meteorological forcing data and initial conditions and approximations in boundary conditions (Liston and Sturm, 1998; Pan et al., 2003). Moreover, there are several physical factors that make an exhaustive reconstruction of snow dynamics complicated: snow intermittence in space and time, stratification and slow phenomena like metamorphism processes, uncertainty in snowfall evaluation, wind transportation (Winstral and Marks, 2014).

Many different snowpack models have been developed with highly variable degree of complexity, mainly depending on their target application, such as hydrological forecasting, avalanche prediction, climate modeling, and the availability of computational resources and data. Snow models range from the so-called force-restore systems of composite snow-soil layer(s) (Douville et al., 1995; Yang et al., 1997) and explicit snow layer(s) schemes (Slater et al., 1998; Verseghy, 1991) up to detailed internal-snow-process schemes with physical parameterizations (Anderson, 1976; Bartelt and Lehning, 2002; Brun et al., 1989; Endrizzi et al., 2014; Jordan, 1991; Lehning et al., 2002; Vionnet et al., 2012). Intermediate-complexity systems result from simplified versions of the physical parameterization schemes with a reduced snowpack layering (Boone and Etchevers, 2001; Dutra et al., 2010, 2012). One of the main issues is the trade-off between model complexity and input data requirements. Independent studies comparing snow models with different scheme complexity agreed in stating that a simplified snowpack structure can provide nearly equivalent performance as a much more complex snow-physics model (Avanzi et al., 2016; Magnusson et al., 2011, 2015). Thus, for many applications, a simpler snowpack scheme may be an optimal compromise between model performance and computational constraints.

Several intercomparison projects aimed at assessing performance of models with different levels of detail and parameterizations with the purpose of analyzing their impact on model simulations (Boone et al., 2004; Bowlinget el., 2003; Essery et al., 2009; Etchevers et al., 2003; Nijssen et al., 2003; Schlosser et al., 2000; Slater et al., 2001). These projects stated that no

overall best model could be identified and an increasing model complexity does not ensure an improvement of simulations, whose quality depends on the application, and topographic, meteorological and vegetation features of the modeling domain (Rutter et al., 2009).

Essery et al. (2013) presented a snow multi-scheme model combining a range of existing parameterizations of different complexity (from empirical to physical ones) for the representation of each dominant process occurring within the snowpack. This approach allows generating a large ensemble of simulations with different model configurations and those employing prognostic equations for snow density and albedo generally revealed the best performance.

Fortunately, in addition to model simulations, other independent snow-related data sources are available, such as ground-based measurements and remotely sensed observations (Barrett, 2003), but both are affected by several limitations. Ground-based snow measurements only provide point values, affected by an instrumental bias and subjected to distortions due to wind action, local topographic features and vegetation interactions. Remote sensing observations cover extended areas but they supply indirect measurements affected by a usually coarse spatial resolution (passive microwave sensors) and the uncertainty in retrieval algorithms.

Data Assimilation (DA) is an objective methodology to combine these different sources of information to obtain the most likely estimate of snowpack state.

Several DA techniques with different degree of complexity have been developed and are currently employed: direct insertion (Liston et al., 1999; Malik et al., 2012; Rodell and Houser, 2004), optimal interpolation scheme (Brasnett, 1999; Liston and Hiemstra, 2008), Cressman scheme (Balsamo et al., 2015; Cressman, 1959; Dee et al., 2011; Drusch et al., 2004), nudging method (Boni et al., 2010; Stauffer and Seaman, 1990).

At a higher level of complexity, Kalman filtering is a class of sequential DA techniques (Evensen, 2003) that enables to evaluate the optimal weighting between modeled and observed states knowing model and observations errors. The main feature distinguishing this approach from more static ones is the dynamic updating of the forecast error covariance during the simulation. Several techniques based on the Kalman filter have been developed.

The standard Kalman Filter (KF) (Gelb, 1974), which can be implemented only on linear dynamic system, is based on the relative contribution of the covariance matrices of the errors of both the model predictions and the observations to obtain a statistically optimal estimate for the given parameters set and assumed uncertainties. This is achieved by applying a standard error propagation theory that produces an analysis state obtained by adding a correction to the a priori state. The correction is computed as the difference between the a priori state (produced by the model) and the observation, modulated through the Kalman Gain, a matrix that resumes the information from both the covariance matrices.

The Extended Kalman Filter (EKF) (Miller et al., 1994) is a linearized statistical approach that can be applied to nonlinear dynamic systems. This technique relies on an adjoint and tangent linear model to propagate the error covariance matrix forward in time. Thus, this technique is able to provide only a near-optimal estimate due to the linear approximation of the model through a Taylor series expansion. Sun et al. (2004) developed a one-dimensional EKF scheme to assimilate synthetically generated Snow Water Equivalent (SWE) observations into a Land Surface Model (LSM). Dong et al. (2007) used the assimilation system developed by Sun et al. (2004) to assimilate SWE data derived from the Scanning Multichannel Microwave Radiometer (SMMR) observations into a LSM. The EKF-based scheme results to well succeed in updating model simulations, even though in presence of strong nonlinearities in the system, unstable results are attended (Moradkhani, 2008).

A further approach is the Ensemble Kalman Filter (EnKF), proposed by Evensen (1994, 2003). Unlike the traditional and Extended Kalman filters, this method does not need a model linearization since the error estimates are evaluated from an ensemble of model simulations using the Monte Carlo approach. Moreover, this method is able to handle any number of variables in the update scheme. Andreadis and Lettenmaier (2005) applied an EnKF scheme to assimilate the Moderate Resolution Imaging Spectroradiometer (MODIS) snow cover extent (SCE) and the Advanced Microwave Scanning Radiometer–EOS (AMSR-E) SWE products into a macroscale hydrologic model to update SWE model predictions. Clark et al. (2006) proposed an alternative framework for assimilating synthetic remotely sensed snow cover area (SCA) data to improve streamflow simulations. Slater and Clark (2006) implemented this technique to assimilate SWE observations to update the snowpack state of a conceptual model. Su et al. (2008) investigated the feasibility of assimilating through the EnKF approach the fractional snow cover (FSC) detected by MODIS for the optimal retrieval of continental-scale SWE within a highly complex LSM. More recently, Magnusson et al. (2014) analyzed the impact of an EnKF-based assimilation of both ground-based SWE observations and snowfall and snowmelt rates on distributed SWE estimates.

All the studies generally state that the EnKF is a well-performing technique enabling to consistently update model predictions. The assimilation of snow-related observations through the EnKF scheme succeeds in improving the analysis of snowpack dynamics, especially during the melting period, with a resulting enhancement of the accuracy of hydrological simulations. Nevertheless, most publications about applications of EnKF-based scheme deal with univariate assimilation, namely the assimilation of a single data type (Griessinger et al., 2016; Huang et al., 2017). Relatively few studies aimed to investigate the simultaneous assimilation of observations of multiple model state variables. Durand and Margulis (2006) assimilated synthetic passive microwave observations at the Special Sensor Microwave Imager (SSM/I) and AMSR-E frequencies and broadband albedo observations through an EnKF scheme to study the potential of remotely sensed snow observations in improving SWE simulations. Durand and Margulis (2008) assimilated synthetic SWE and snow grain size data with different spatial resolutions into a LSM using adaptive EnKF. Su et al. (2010) developed a multisensory EnKF-based DA system assimilating both Gravity Recovery and Climate Experiment (GRACE) terrestrial water storage (TWS) and MODIS FSC with respectively the EnK Smoother (Dunne and Entekhabi, 2005, 2006) and EnKF into a LSM. De Lannoy et al. (2012) studied the impact of the joint assimilation of AMSR-E SWE and MODIS FSC products on SWE simulations with a multiscale EnKF scheme. More recently, Stigter et al. (2017) proposed a well-performing EnKF-based methodology to estimate SWE and snowmelt runoff in a Himalayan catchment. They implemented an EnKF scheme to calibrate ruling parameters of a snow model by jointly assimilating both remotely sensed snow cover observations and ground-based measures of snow depth. Current research results agree on the superior impact of the multivariate assimilation on model simulations with respect to the univariate one (Charrois et al., 2016). However, even though in atmospheric sciences the multivariate

DA is well established, most publications in the framework of terrestrial systems present synthetic case studies (Montzka et al., 2012).

In light of the promising potential of multivariate DA schemes and the lack of their application using real-world data or several types of data, this paper intends to investigate the feasibility of a multivariable EnKF-based scheme for snow modeling. The main goal is the development of a operationally effective system enabling to assimilate both ground-based measurements and remotely sensed data of several snow-related variables (surface temperature, snow depth and albedo). Since multivariate DA systems are usually very CPU-intensive, the research aims to define and analyze technical solutions and approaches allowing to reduce the required computational load by still guaranteeing successful performance. To this end, several sensitivity experiments were carried out in order to better understand system robustness and reliability.

The paper is organized as follows. Firstly, the snow dynamic model and the DA algorithm are described. After presenting the ground-based and remote sensed data used in the assimilation experiments, the experimental design is explained, whose results are then shown and widely discussed.

SMASH – SNOW MULTIDATA ASSIMILATION SYSTEM FOR HYDROLOGY

This research aimed to develop a snow modeling system suited to real-time applications and able to combine model predictions, ground-based data and satellite observations.

SMASH (Snow Multidata Assimilation System for Hydrology) consists of a multi-layer snowpack dynamics model that reproduces some of the main physical processes occurring within the snowpack (accumulation, density dynamics, melting, sublimation, radiative balance, heat and mass exchanges), and a multivariable DA algorithm.

Snow hydrological model

From a hydrological point of view, the most relevant quantities to be predicted are the SWE and the snowmelt. The evolution of snow microstructure, snowpack stratification, and snow metamorphism are ruling processes for the avalanches forecasting (Bartelt and Lehning, 2002; Vionnet et al., 2012) but they are of less interest in most hydrological applications, and thus they are here neglected. Since the aim is to develop a snow model suitable to be coupled with a multivariable DA algorithm, the degree of model complexity is limited in order to facilitate the assimilation procedure while maintaining a fundamental physical consistency (Magnusson et al., 2014; Slater and Clark, 2006). This purpose leads to some model simplifications of both snowpack scheme and physics (liquid water storage and refreezing process are not included). The introduction of a finer layering scheme with respect to the simple discretization described below would add a further challenge in the assimilation of observed data through DA techniques involving state-averaging operations. The implementation of an EnKF scheme would be much more demanding since a higher number of layers (i.e. increased state size) entails larger computational requirements.

The multilayer scheme consists of a 2-layers discretization for snowpack and 2-layers for soil (Figure 1). The scheme has a seasonally variable number of layers ranging from a minimum of two, in snow free condition, up to a maximum of four layers, in presence of snow cover. This dynamic layering scheme is adopted with the aim to solve the model energy balance in both snowy and snowless conditions without having to rely on a 'model switching' algorithm. Both snow and soil upper layers are much thinner than the underlying ones so that the top layer temperature can be considered as an acceptable approximation of the skin temperature, whose measures can be more efficiently assimilated. The model is driven by meteorological data (air temperature, wind velocity, relative air humidity, precipitation and incident shortwave solar radiation) to provide a complete estimate of snowpack state in an explicit surface energy balance framework. Model state consists of snow surface temperature (T_s [°C]), snow temperature at the interface between the two snow layers (T_m [°C]), surface soil temperature (T_0 [°C]), deep soil temperature (T_d [°C]), SWE and snow density of top (W_s [mm]; ρ_s [kg/m^3]) and bottom (W_m [mm]; ρ_m [kg/m^3]) snow layers, surface albedo (α [–]).

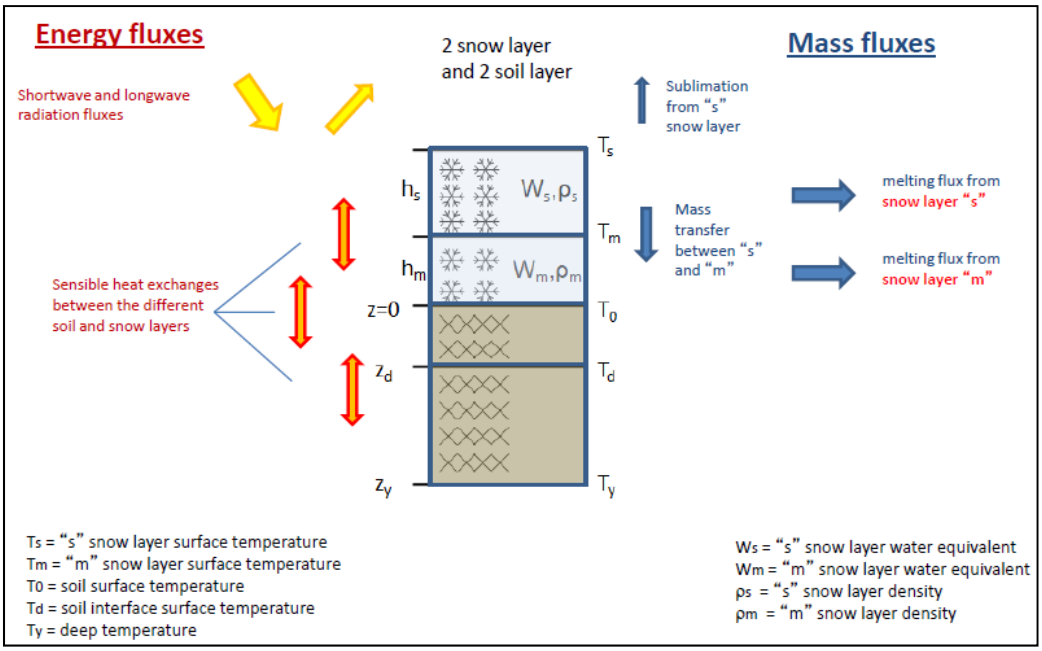

Fig. 1. SMASH scheme - Energy and mass fluxes between adjoining layers and atmosphere are shown.

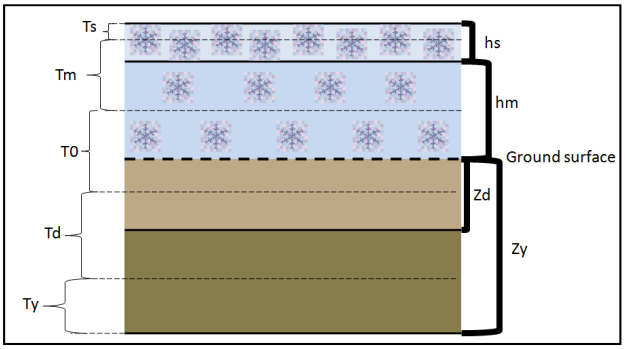

Fig. 2. SMASH scheme - Control volumes and model layers.

The thicknesses of soil layers are fixed through reference depths at 30 cm and 2 m (z_d and z_y). Snow layers vary their thickness (h_s and h_m) according to the snow dynamics (i.e. snowfalls, sublimation, density changes, and snow melting) without any constraining limit. Deep soil temperature (T_y) is the model boundary condition. Temperatures (T_s, T_m, T_0, T_d) are defined as average temperatures of the control volumes shown in Figure 2. The top and bottom boundaries of each volume are set in the middle of the thickness of the two corresponding consecutive layers.

The model solves both energy and mass balance with an integration time step of 15 minutes.

Mass balance

Snow mass balance equations evaluate SWE of each snow layer (W_s and W_m) accounting for snowfalls (Sf), sublimation process ($subl$), melting rates from both the two snow layers (M_s and M_m) and mass transfer between them (D). Since neither the liquid storage nor the refreezing process is included within the snowpack model, meltwater is assumed to be drained directly as surface runoff (no infiltration into the soil).

$$W_s(t) = W_s(t-1) + Sf - M_s - subl - D \tag{1}$$

$$W_m(t) = W_m(t-1) + D - M_m - subl \tag{2}$$

$$D = \frac{1}{X} W_s dt \tag{3}$$

The mass transfer (D) from the snow surface layer downward is empirically parameterized as a function of the SWE and a temporal scale of the process (X). This parameter was properly defined through several tests at different measurements sites in order to obtain a constant value allowing to maintain a thin snow surface layer. From a physical point of view, this parameterization can be supposed to contribute to the gravitational snowpack settling thanks to a consistent update of the snow density of both the snow layers.

Given the observed total precipitation, the snowfall rate (Sf) is evaluated as a function of air temperature (T_a) and relative humidity (U), as proposed in Froidurot et al. (2014).

Density

Snow density is updated considering both the snow compaction and the destructive thermal metamorphism according to the parameterization proposed by Anderson (1976). The snow compaction is evaluated as the ratio between the weight of the overlying snow (σ_{si}) and a viscosity coefficient (η_{si}) standing for the snow resistance to a certain pressure and evaluated as an exponential function of snow temperature and density (Kojima, 1967; Mellor, 1964). The thermal metamorphism is estimated as a function of snow temperature (T_{si}) and density (ρ_{si}). The influence of settling is higher in new snow layers (50–150 [kg/m^3]) up to a density value of 250 [kg/m^3].

$$\frac{1}{\rho_{si}} \frac{d\rho_{si}}{dt} = \frac{\sigma_{si}}{\eta_{si}(T_{si}, \rho_{si})} + \xi_i(T_{si}, \rho_{si}) \tag{4}$$

In case of snowfall, snow density of the upper layer is evaluated as a weighted average between its current value and fresh snow density. The fresh snow density is evaluated according to the air temperature (Hedstrom and Pomeroy, 1998).

Energy balance an d heat flow

The model evaluates the net heat fluxes in each layer and the conductive heat fluxes between adjoining layers according to Fourier law. The surface heat flux ($\vec{G}$) is estimated as the resulting balance among shortwave and longwave radiations $\left(\vec{R}_{Sw,net}, \vec{R}_{Lw,net}\right)$, sensible $\left(\vec{H}\right)$ and latent $\left(\overrightarrow{LS}\right)$ heat fluxes, and the advection heat flux $\left(\vec{Q}_{mix}\right)$ due to liquid precipitation:

$$\vec{G} = \vec{R}_{Sw,net} + \vec{R}_{Lw,net} + \vec{H} + \overrightarrow{LS} + \vec{Q}_{mix} \tag{5}$$

Both the incoming (positive) and outgoing (negative) longwave radiation components are estimated through the Stephan-Boltzmann law, as a function of the surface temperature (i.e. the temperature of snow/soil depending on the presence/absence of snow cover) and the air temperature, respectively. While the surface emissivities are considered as constant values, the air emissivity varies over time according to both wind speed and air temperature.

The heat flux from liquid precipitation across the snowpack surface is a function of rain emissivity (ε_p), the surface specific heat (C_s), the amount of rain (P_l) and the temperature gradient:

$$Q_{mix} = \frac{\varepsilon_p C_s P_l \left(T_a - T_{sup}\right)}{dt} \tag{6}$$

The net shortwave radiation ($R_{Sw,net}$) is evaluated as a fraction of the incident solar radiation ($R_{Sw,inc}$), as a function of the surface albedo (α):

$$R_{Sw,net} = (1-\alpha) \cdot R_{Sw,inc} \tag{7}$$

In snow cover condition, the albedo is evaluated through a physical parameterization (Wiscombe and Warren, 1980):

$$\alpha = \alpha_d + 0.2(1-\alpha_d) \tag{8}$$

$$\alpha_d = (1 - 0.2 F_{AGE}) \cdot \alpha_0 \tag{9}$$

where α_d is the diffuse albedo and $\alpha_0 = 0.95$. Since snow albedo decreases with time due to the growth of snow grain size and accumulation of dirt, a reduction factor is parameterized according to the snow age (τ_{snow}):

$$F_{AGE} = \frac{\tau_{snow}}{1 - \tau_{snow}} \tag{10}$$

In case of snowfall, the snow age is reduced, hence the surface albedo.

The penetration of shortwave radiation into the snowpack is estimated after Anderson (1976). According to this formulation the solar radiation decays exponentially as a function of snow depth.

$$R_{Sw\downarrow} = R_{Sw,net} \cdot \exp(-\nu \cdot z) \quad (11)$$

where:

- $R_{Sw\downarrow}$ is the fraction of solar radiation penetrated withinthe snowpack;
- $R_{Sw,net}$ is the net shortwave radiation on the snowpack surface;
- $\nu$is the extinction coefficient [cm^{-1}];
- z is the penetration depth [cm];

Sensible and latent heat fluxes are evaluated following the bulk formulation:

$$H = c_p \rho_a C_H V (T_{sup} - T_a) \qquad \textit{Sensible heat flux} \quad (12)$$

$$LS = L_H \rho_a C_H V (q_{sup} - q_a) \qquad \textit{Latent heat flux} \quad (13)$$

Heat exchanges are proportional to the temperature (for H) and mixing ratio (for LS) gradients between the surface (T_{sup} and q_{sup}) and atmosphere (T_a and q_a). Turbulent fluxes are also function of air specific heat (c_p), latent heat (L_H) of sublimation (of vaporization when no snow cover is present), air density (ρ_a), wind velocity (V) and the turbulent transfer coefficient (C_H). The turbulent transfer coefficient C_H depends on the neutral conditions coefficient C_{HN}, evaluated as a function of the surface roughness, and the atmospheric stability (ψ_{stab}):

$$C_H = C_{HN} \psi_{stab} \quad (14)$$

The atmospheric stability is evaluated as a function of the Richardson Bulk number, which depends on potential temperatures of both air and interface surface between soil/snow and atmosphere and wind velocity, following the empirical scheme of Caparrini et al. (2004).

Temperature variation in time (ΔT_i) and snow melting rate (M_i) of each layer is evaluated as a function of the net heat flux (Q_{Ti}): at its surface, resulting from the balance of conductive fluxes among layers and the contribution of the penetration of solar radiation:

$$\Delta T_i = \frac{Q_{Ti}}{h_i \rho_i C_i} dt \quad \text{If } T_i > T_{melt} \rightarrow M_i = \frac{Q_{Ti\_melt}}{L_m} dt \quad (15a, b)$$

where C_i is the specific heat of the layer. When the resulting temperature of the layer (T_i) exceeds the melting temperature (T_{melt} = 0°C), melting occurs in the corresponding control volume (M_i) according to the equation [15b], where L_m is the melting latent heat.

Model calibration

The snowpack model was calibrated over four winter seasons (2012/13 – 2013/14 – 2014/15 – 2015/16) through a split-sample test. A sensitivity analysis allowed to properly select the parameters exerting the most influence on model simulations. This preliminary study was manually carried out by making the parameters vary within proper ranges and analyzing the impact of their variation on the resulting model predictions. Two model parameters were selected: snow roughness and snow viscosity. Parameters ranges were estimated in order to both avoid model numerical instabilities and to comply with possible physical constraints (see Table 1). Random combinations of parameters were tested by analyzing the resulting Kling-Gupta efficiency (KGE) indices (Gupta et al., 2009) considering the observations of surface temperature, snow depth, and albedo supplied by the Torgnon station and the monthly manual measures of snow density. Starting from the best parameters combinations, local KGE optima were found over the calibration period (winter seasons 2012/13–2013/14) through a constrained nonlinear optimization algorithm (Interior-point Algorithm) (Wächter and Biegler, 2006) in order to define the best parameters set. Finally, the calibrated parameters were tested throughout the validation period (snow seasons 2014/15 – 2015/16). Table 2 shows the resulting KGE values over both calibration and validation periods.

Table 1. Parameters calibration.

	Parameter		Range	Calibrated value
1.	Snow roughness	[mm]	[0.001–0.05]	0.0226
2.	Snow viscosity	[kg/ms]	[10^6–10^8]	10^8

Table 2. Kling-Gupta efficiency coefficients over both calibration and validation periods.

	Kling-Gupta efficiency	
	Calibration period	Validation period
Snow depth [m]	0.74	0.69
Snow temperature [°C]	0.58	0.54
SWE [mm]	0.12	0.51

Data assimilation algorithm: constrained Ensemble Kalman filter

An Ensemble Kalman Filter scheme is implemented to assimilate observations of surface temperature, snow depth, and albedo. This technique requires the definition of an ensemble of model states, which are all simultaneously integrated forward in time independently of each other. Whenever an observation is available, the states of the ensemble members are updated through an optimal weighting between simulated and observed values. The weights are defined by the Kalman Gain (K), based on the covariance errors matrices of both model and observations. Model error covariances are dynamically updated at every assimilation time step (Evensen, 1994, 2003). The model state correction formula, i.e. the state analysis, is defined as:

$$x_{analysis} = x_{background} + K \cdot (obs - H \cdot x_{background}) \quad (16)$$

where $x_{analysis}$ is the updated model state, $x_{background}$ is the prior one, i.e. the model predictions, and obs are the observations. The Kalman Gain is a linear combination of the covariance errors matrices of both model (C_{mod}) and observations (C_{obs}) and a measurement operator (H), which enables the transition from the model space to the observations one (Evensen, 1994).

$$K = C_{mod} H^T \left(H C_{mod} H^T + C_{obs} \right)^{-1} \quad (17)$$

According to the main assumptions of the EnKF formulation (Evensen, 1994), model errors covariance matrix (C_{mod}) is the covariance matrix of the differences between each ensemble state (Ens_i) and the resulting average ensemble state (Ens_{mean}):

$$C_{mod} = Cov\left(Ens_i - Ens_{mean}\right) \quad (18)$$

The correlations among state variables of a highly non-linear model may be difficult to assess through simple ensemble statistics, with possible miscorrection of the model background errors, especially for those state variables which are not directly observed. In order to overcome some of these limitations and obtain an overall consistent update of the snowpack state, the model error covariance matrix is reduced to a two-blocks structure. The two blocks handle the covariances among energy- and mass-related variables independently. The implementation of this solution allows updating both energy and mass balances by limiting physically incoherent corrections. Furthermore, with the aim of avoiding possible model instabilities, any inconsistent value generated through the ensemble updating is removed by limiting each state variable into proper variables physical ranges. According to this approach, any outlier value is set equal to upper or lower limit value of the corresponding physical range of the state variable.

Ensemble Gaussian perturbations

Because this study mainly focuses on assessing the performance of a multivariable DA scheme, perturbations are restricted to the ensemble of model states. Indeed, observations are here assumed to be significantly more reliable than model predictions. The observations error covariance matrix is estimated according to the instruments uncertainties (Table 3). Since the measurements of each observed variable are here considered independent of each other, the resulting error covariance matrix is diagonal. Of course, point measurements have high uncertainties due to their limited representativeness of the spatialized snow processes (e.g. wind-driven snow redistribution) (Stigter et al., 2017). However, since this is a point application of the DA scheme, the observational error covariance matrix is supposed to be satisfactorily representative even though any other source of uncertainty is included. The uncertainty of forcing meteorological data is not taken into account.

Table 3. Uncertainties of the assimilated measures.

Observed variable	Measures uncertainty
Surface temperature [°C]	±0.5
Snow depth [cm]	±1
Albedo [%]	5

State variables are perturbed at each model time step through an additive Gaussian noise. The perturbations are generated by performing, for each state variable, a Gaussian sampling from a normal multivariate distribution with an assigned covariance matrix (De Lannoy et al., 2012). This latter prevents the introduction of possible inconsistencies among the variables of each model state due to its perturbation. The covariance matrix is evaluated as the error covariance matrix between simulated and observed time series of the state variables, when available. The sampling is carried out by choosing equidistant cumulated probability values, in order to guarantee null mean-valued perturbations and the Gaussianity even if sample size is limited. As well as the model ensemble update, also its perturbation can cause physically inconsistent values.

In this occurrence the aforementioned approach is not relevant, since the truncation of the perturbed ensemble would compromise the null mean-valued perturbations. In order to avoid the insertion of possible distortions, the model physical consistency is guaranteed by rescaling the perturbed ensemble.

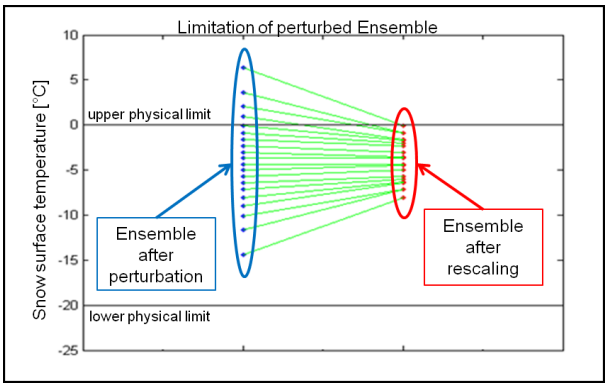

Fig. 3. Ensemble limitation after the perturbation.

This contraction allows maintaining the ensemble average and perturbations Gaussianity even after the ensemble limitation (Figure 3). These two approaches to limiting the perturbed ensemble within physical ranges are compared in the following.

In spite of the perturbation of the model states, the constraints necessarily decrease the variance of ensemble state variables, whose reduction can lead to weight more the model and weakly assimilate the observations. Thus, at each assimilation time step the model error variances are rescaled proportionally to the variance reduction with respect to the empirical variance of each state variable:

$$Cov_{mod} = Corr_{mod} \cdot \left(\sigma_{rescaled} \mathrm{x}\ \sigma_{rescaled}\right) \quad (19)$$

where:

- $Corr_{mod}$ is the model error correlation matrix;
- $\sigma_{rescaled}$ is the vector of the rescaled standard deviations of state variables.

Model physical consistency: modulating function

The model was designed to simulate the energy balance in both snowy and snowless conditions. Thus, in order to guarantee the model consistency both in case of presence and absence of snowpack, two different sets of physical limits are required to constrain each state variable into proper seasonal ranges. These ranges are statistically defined through the analysis of observed time series of the state variables (see Table 4). Moreover, the lower and upper physical limits have to be time variant, in order to well characterize the transition periods (early winter, melting season).

Table 4. Physical ranges to limit the state variables after their perturbation.

Variable		Lower limit		Upper limit	
		Snowy	Snowless	Snowy	Snowless
T_s	[°C]	–30	–	0	–
T_m	[°C]	–30	–	0	–
T_0	[°C]	–10	0	0	40
T_d	[°C]	–2	0	5	20
W_s	[mm]	0	–	–	–
W_m	[mm]	0	–	–	–
ρ_s	[kg/m^3]	80	–	550	–
ρ_m	[kg/m^3]	80	–	550	–
α	[–]	0.2		1	

Since the intermittent presence of snow cover also entails a seasonal variability of state variables correlations, also the error

covariance matrix employed to generate perturbations must be time variant. Indeed, in case of bare soil, snow-related variables are not included in the model state, and some variables are weakly correlated (e.g. deep soil temperature and albedo). In order to generate proper perturbations in snow and no-snow conditions, two different error covariance matrixes are used.

With the purpose of preventing model instabilities a modulation was introduced in order to relax the switch from snow cover to bare soil conditions, by properly setting upper and lower physical limits of the state variables and the error covariance matrix for the generation of ensemble perturbations.

The modulating function (β) allows discriminating the presence or absence of snow according to both air temperature (observed) and snow mass (modeled). This approach enables to manage the transition periods: snow cover and high air temperature (melting process) and bare soil and low air temperature (early winter). The β-function is defined according to the following formulas:

$$\beta_{Ta} = \left(\gamma - \frac{\operatorname{atan}(T_a)}{\pi} \right) \tag{20}$$

$$\beta = \beta_{Ta} + (1 - \beta_{Ta}) \cdot e^{-\left(1+\left(\frac{(W_S + W_m) - \mu}{\sigma}\right)\xi\right)^{-1/\xi}} \tag{21}$$

The functional form and the parameters were chosen to center the function on an air temperature value that could discriminate snow and no-snow conditions, assumed equal to 0°C, and asymptotically reach the desired limit values (1 for winter and 0 for summer).

Figure 4 shows the modulating function, which assumes values near to 0 when air temperature is high and there is no snow cover (mainly during summer season), and near to 1 in case of snow cover and cold temperatures (winter period). In these two limit cases, respectively summer and winter, physical ranges are assumed for all the state variables. The function assumes value near to 1 also when no snowpack is present but temperatures are very low (autumn, early winter). During transition periods β-function allows defining intermediate model run settings according to the combination of snow and air temperature information.

$$Lim_{i,SUP} = \left(Lim_{i,SUP_{snowless}} \cdot (1 - \beta) \right) + \left(Lim_{i,SUP_{snowy}} \cdot \beta \right) \tag{22}$$

$$Lim_{i,INF} = \left(Lim_{i,INF_{snowless}} \cdot (1 - \beta) \right) + \left(Lim_{i,INF_{snowy}} \cdot \beta \right) \tag{23}$$

$$COV_{pert} = \left(COV_{pert,snowless} \cdot (1 - \beta) \right) + \left(COV_{pert,snowy} \cdot \beta \right) \tag{24}$$

where $Lim_{i,SUP}$ and $Lim_{i,INF}$ are the modulated upper and lower physical limits of each state variable and COV_{pert} is the modulated error covariance matrix used to generate the ensemble perturbations.

CASE STUDY

Validation site and ground-based measurements

SMASH 1D-version was tested throughout the period June 2012–December 2013 at the Torgnon measurement site (Tellinod, Aosta Valley, 45.84°N, 7.58°E). The site is a subalpine grassland located in northwestern Italian Alps, at an elevation of 2160 m a.s.l. The area is characterized by a typical subalpine climate, with an average annual temperature of around 3°C and an average annual precipitation of 880 mm. Further details on the study site can be found in Galvagno et al. (2013) and Filippa et al. (2015).

Since 2008, an automatic weather station provides 30-min averaged records of different meteorological parameters, including air and surface temperatures (HMP45, Vaisala, SI-111 and therm107, Campbell Scientific), short- and longwave radiations and surface albedo (CNR4, Kipp & Zonen), precipitation (OTT Pluvio2, Weighing Rain Gauge), soil water content (CS-616, Campbell Scientific), snow depth (SR50A-L, Campbell Scientific) and wind speed (WINDSONIC1-L, Campbell Scientific). Monthly manual measures of snow density (snow pits) are available during the winter season.

Remotely sensed observations

With the aim of evaluating the impact of the assimilation of remote sensed observations, the assimilation of Land Surface Temperature (LST) supplied by the Meteosat Second Generation (MSG) mission was introduced instead of the surface temperature locally measured by ground-based sensor. LST is the radiative skin temperature over land, whose retrieval is based on clear-sky measurements from the Spinning Enhanced Visible and InfraRed Imager (SEVIRI) aboard the geostationary MSG satellite (Jimenez-Munoz and Sobrino, 2008). Since this is a multi-spectral sensor, imaging across the visible and near-IR,

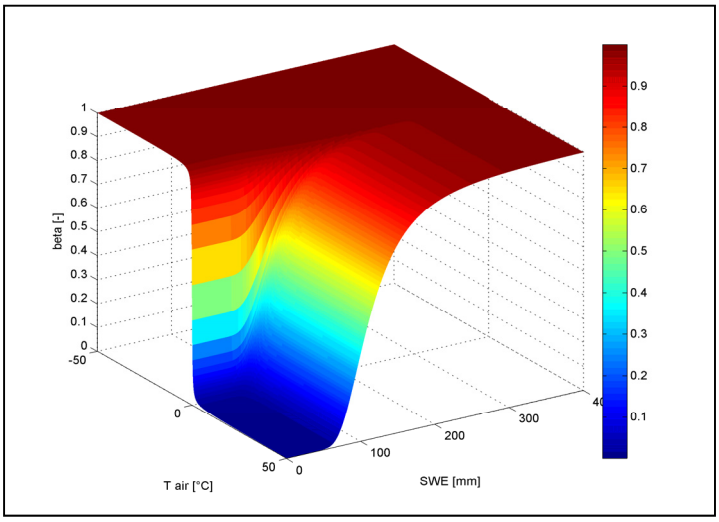

Fig. 4. Beta modulating function.

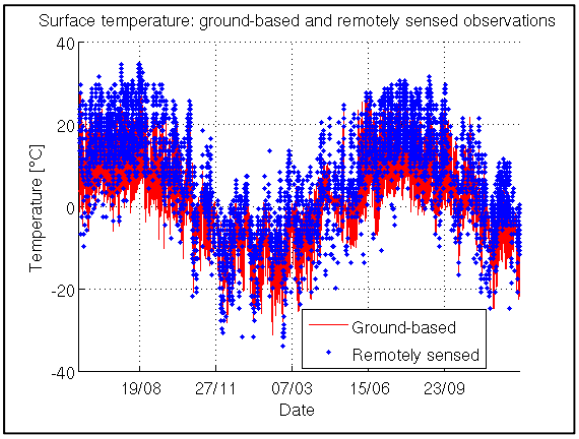

Fig. 5. Time series of ground-based and remotely sensed observations of surface temperature.

LST data are not available in cloudy condition. Despite the coarse spatial resolution of 5–6 km at the latitude of the study area, the temporal resolution of 15 minutes guaranteed by SEVIRI sensor can allow a significant reduction of the cloud cover affecting the remote sensed observations. Moreover the 15 minutes sampling makes this satellite product well suited to being employed in the DA procedure. Compared to the ground-based measurements of surface temperature at the Torgnon site, remote sensed LST is affected by a bias of about +5°C (see Figure 5), even though the two time series are well correlated (correlation coefficient equal to 0.85). A large fraction of the difference between the MSG LST and the ground-based one may be due to the kilometer-size footprint of the satellite product on a steep region where the spatial gradient of LST is of the order of degrees per kilometer.

EXPERIMENTS

Control experiments

DA impact on the accuracy of model simulations was evaluated by using an ensemble of 20 model states. Every 3 hours the in-situ data of the following variables were assimilated: surface temperature, snow depth and albedo. In the first control experiment the assimilated surface temperature observations were provided by the ground station (Exp_c1), while in the second one were supplied by MSG satellite (Exp_c2). With the aim of assessing the relative performance of DA, an open-loop simulation (no DA) is considered as control run.

Sensitivity experiments

With the purpose of analyzing SMASH performance and its sensitivity to different data assimilation settings, several experiments were carried out. Sensitivity to DA frequency was tested by assimilating the available observations every 3, 6, 12, 24 hours (Exp_s1). Sensitivity to ensemble size was evaluated by varying the number of ensemble members from 6 to 100 (Exp_s2). Moreover, the impact of the assimilation of different observed variables was investigated by assimilating different combinations of them (Exp_s3):

a. Only surface temperature (T_{sur});
b. Only snow depth (H_s);
c. Only albedo (Alb);
d. Surface temperature and snow depth (T_{sur} + H_s);
e. Surface temperature and albedo (T_{sur} + Alb);
f. Snow depth and albedo (H_s+Alb).

Since the aim is to assess the performance of the snow-related multivariable DA scheme, the experiments results are shown in terms of snowpack surface temperature, snow depth and SWE during the winter season to evaluate its efficiency in jointly updating several observed variables. Results are restricted to the winter period since in snowless conditions the DA scheme is limited to assimilation of only surface temperature.

Each experiment was quantitatively analyzed through the following statistical metrics, by considering the total amount of measurements, available every 30 minutes. Indirect SWE observations were retrieved from the monthly measures of snow density and the corresponding snow depth ones.

$$R = \frac{cov(Obs, Exp)}{\sigma_{obs} \cdot \sigma_{exp}} \qquad \text{Correlation coefficient (R)} \qquad (25)$$

$$RMSE = \sqrt{\frac{1}{N}\sum_{k=1}^{N}(Obs_k - Exp_k)^2}$$

Root Mean Square Error (RMSE) (26)

$$NER = \left(1 - \frac{RMSE_{Exp}}{RMSE_{OL}}\right) \cdot 100$$

Normalized Error Reduction (NER, Chen et al., 2011) (27)

$$Eff = \left(1 - \frac{\sum_{k=1}^{N}(Exp_k - Obs_k)^2}{\sum_{k=1}^{N}(OL_k - Obs_k)^2}\right) \cdot 100$$

Assimilation efficiency (Eff, Brocca et al., 2012) (28)

RESULTS

Control experiments

Exp_c1

Figure 6, Figure 7 and Figure 8 show the results of the Exp_c1. The open loop simulation (model run without assimilation) generally reveals an underestimation of the diurnal surface temperature peaks and a significant overestimation of the nocturnal ones. Indeed, even though the simulation gets the daily thermal cycle, it fails in reproducing the size of the temperature range. The model well represents the seasonal snowpack dynamics also in the open loop simulation, which results to be not affected by any significant bias. An overestimated snow compaction results in a underestimation trend during the accumulation period. Even though only a few SWE observations are available (monthly indirect measures), the model reveals a general underestimation of the snow mass. The multivariable DA scheme succeeds in forcing the average of the model states ensemble towards the observed values both in terms of surface temperature and snow depth. When considering the DA impact on SWE simulation, it is important to consider that no direct measurement of this variable is assimilated. However, through the multivariable DA the filter well succeeds in consistently updating the prediction of SWE dynamics with a resulting reduction of the underestimation during the accumulation period and a faster snow melting. Table 5 shows the improvement of snow depth simulations with a RMSE decrease of about 8 cm and an approximately unit correlation. Surface temperature is enhanced with a RMSE reduction of around 1°C and a resulting higher positive correlation. Despite of a poor sample, the statistical indices show that the assimilation of snow data allows a drop of the SWE RMSE of about 10 mm with a slight worsening of the correlation, which still maintains a high positive value.

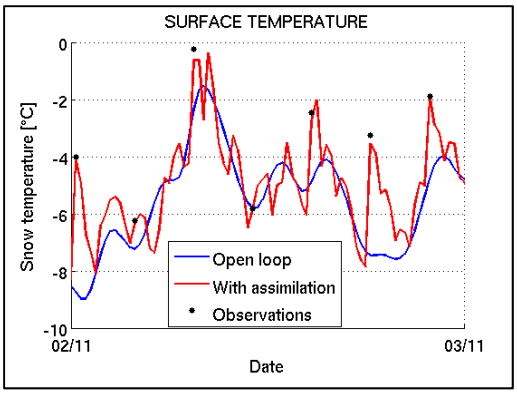

Fig. 6. Exp_c1 - Snow temperature time series 02nd - 03rd November 2012.

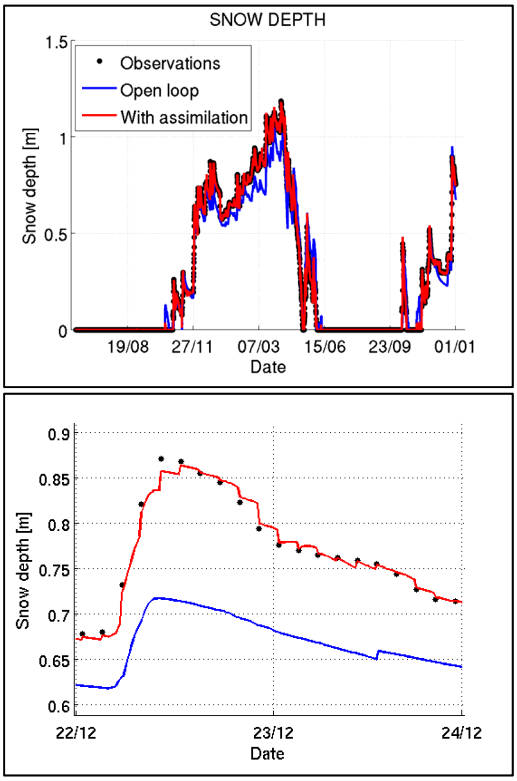

Fig. 7. Exp_c1 - Snow depth time series throughout the analysis period (top panel); Zoom from 22nd- 24th December 2012 (bottom panel).

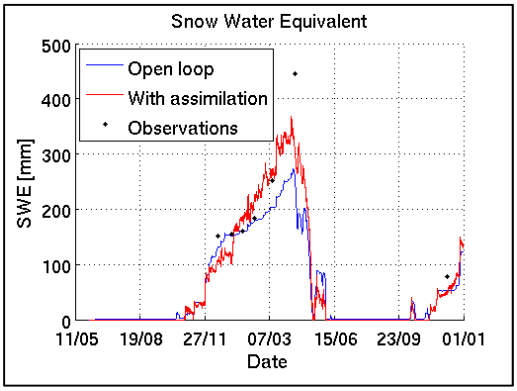

Fig. 8. Exp_c1 – SWE time series throughout the analysis period.

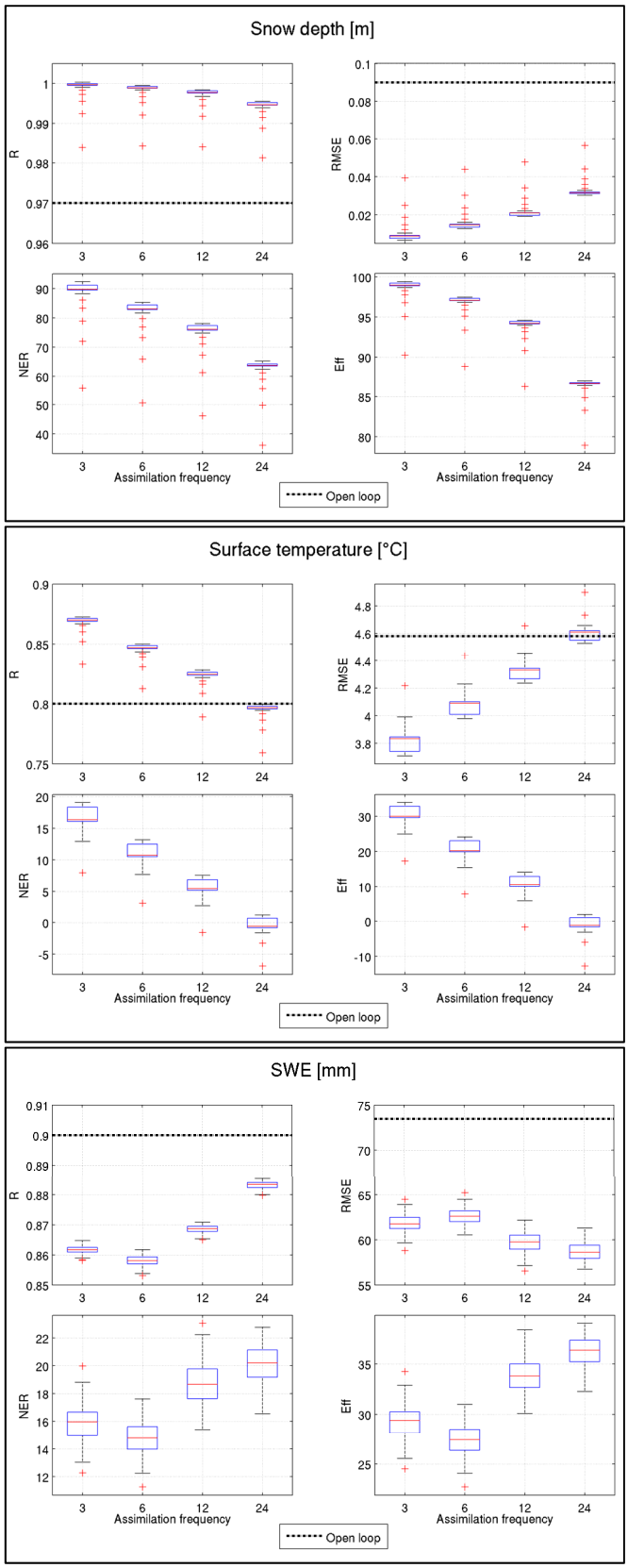

Fig. 9. Exp_s1 – Variable assimilation frequency for: a) snow depth, b) snow temperature, c) SWE.

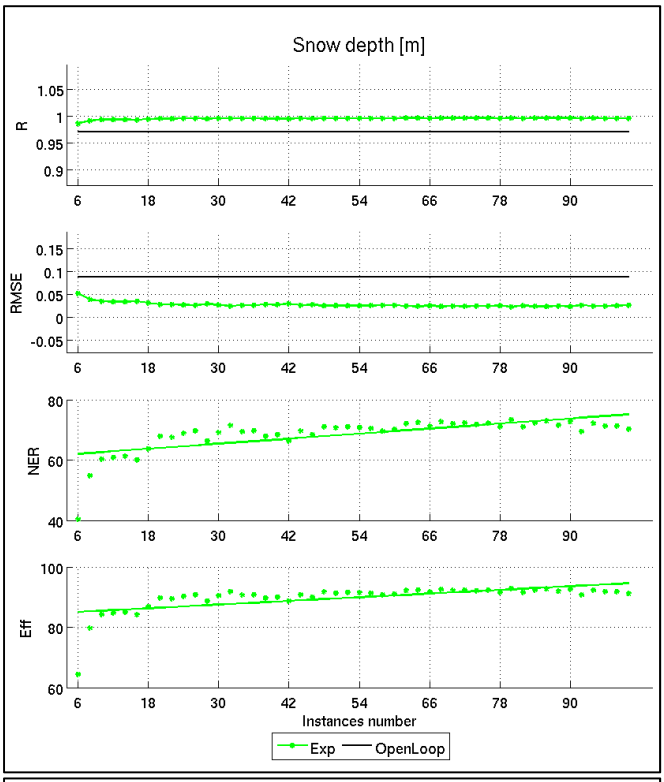

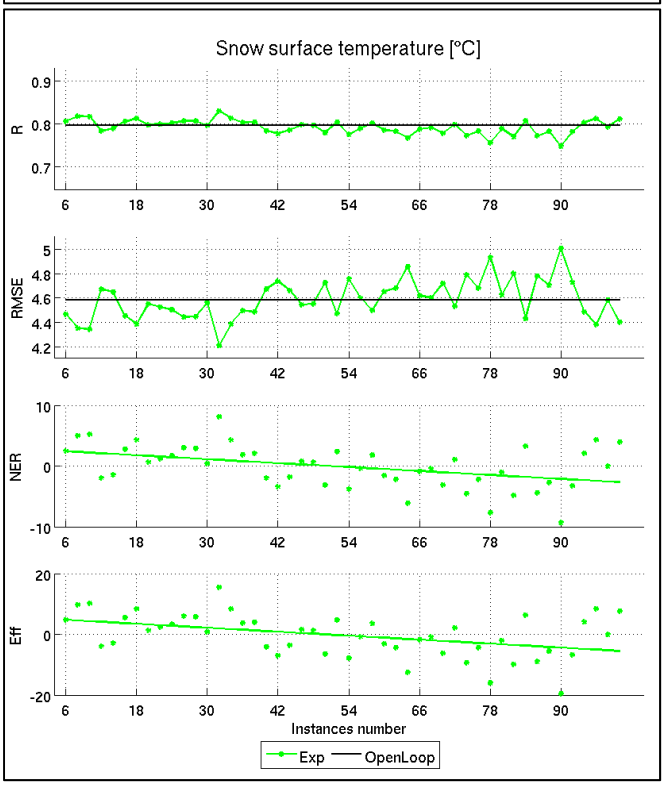

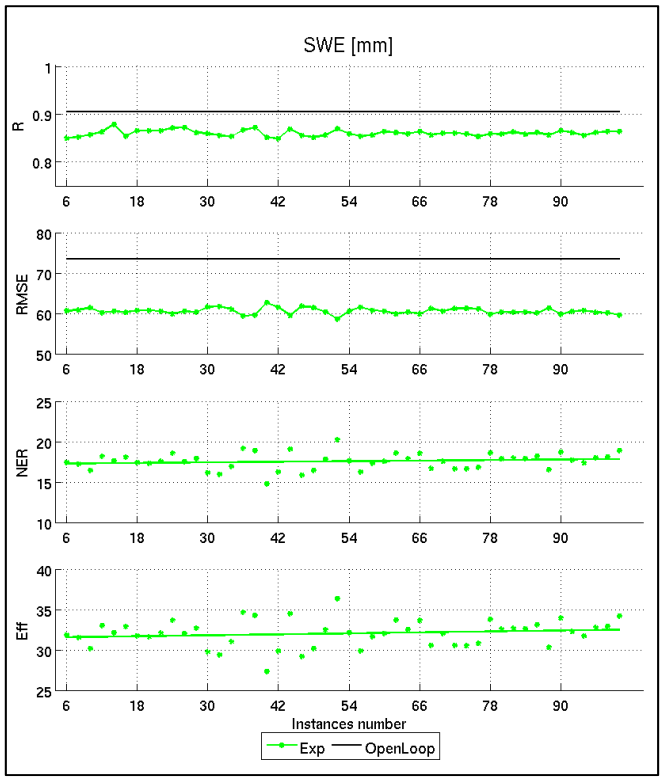

Fig. 10. Exp_s2 – Variable ensemble size for: a) snow depth, b) snow temperature, c) SWE.

Exp_c2

Table 5 shows the results of the joint assimilation of ground and satellite-based observations (Exp_c2). Since the remote sensed LST revealed an important bias, it is assimilated with a properly higher uncertainty with respect to the ground-based measurements. As expected, the overestimation affecting the satellite observations weakens the temperature simulation with a RMSE increase of about 0.5°C and poorer correlation with respect the open loop one. Nevertheless, the model performances are improved in terms of snow depth, whose RMSE decreases to less than 1 cm with an approximately unit correlation. Likewise, the multivariable DA well succeeds in improving the SWE simulations despite of the larger bias affecting the temperature observations.

Sensitivity experiments

Exp_s1

The system sensitivity to the assimilation frequency is shown in Figure 9. Statistical metrics reveal a foreseen worsening of filter performance in updating the directly assimilated variables (surface temperature and snow depth) as the assimilation frequency decreases. For these variables the 3-hours assimilation generally guarantees the best improvement. As expected, snow depth simulation (Figure 9a) is less sensitive to the assimilation time step than the temperature one (Figure 9b), mainly

Table 5. Exp_c1 and Exp_c2 – Statistical indices.

			Control experiments							
	Open loop		Exp_c1				Exp_c2			
Scores	Corr	RMSE	Corr	RMSE	NER	Eff	Corr	RMSE	NER	Eff
Snow depth [m]	0.97	0.09	0.99	0.01	88.52	98.68	0.99	0.01	89.23	98.84
Snow temperature [°C]	0.80	4.58	0.87	3.85	16.07	29.56	0.75	5.01	–9.33	–19.54
SWE [mm]	0.90	73.46	0.86	62.46	14.98	27.71	0.86	60.27	17.97	32.71

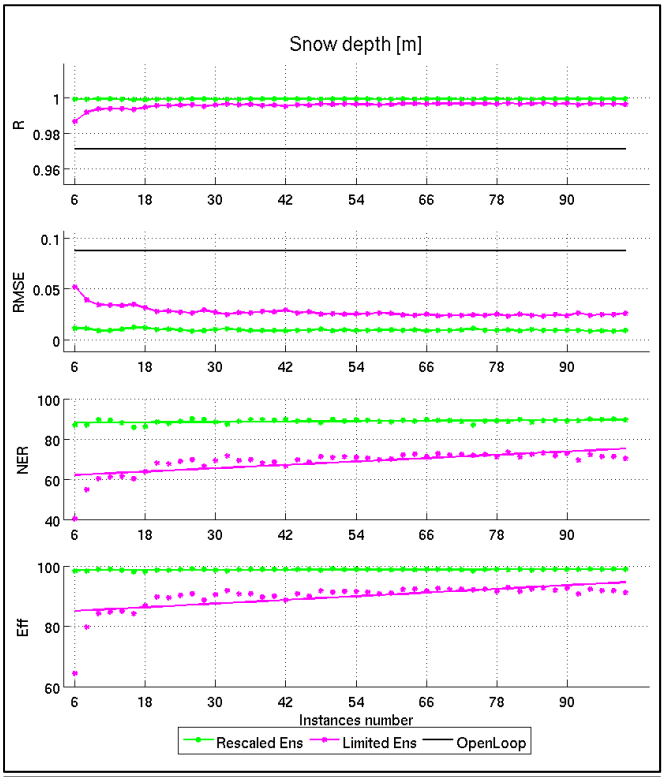

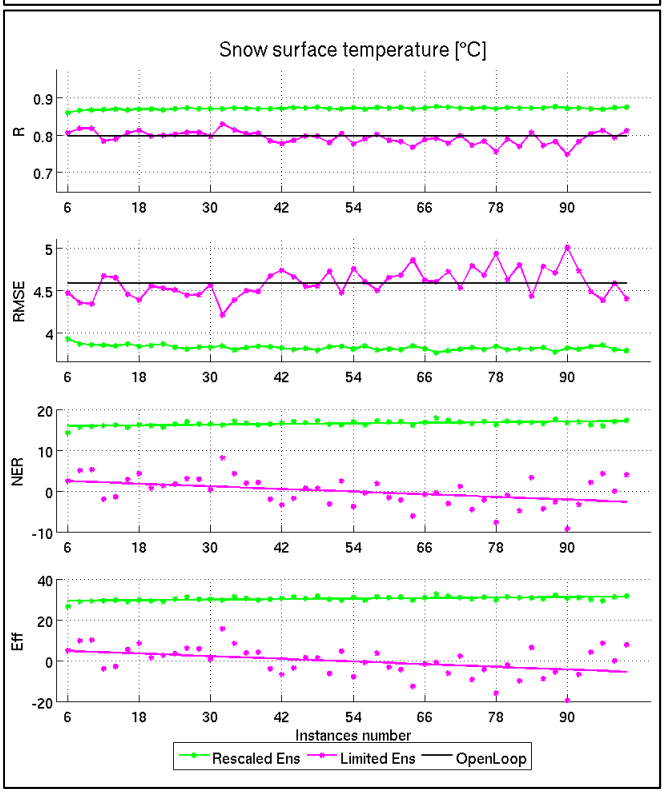

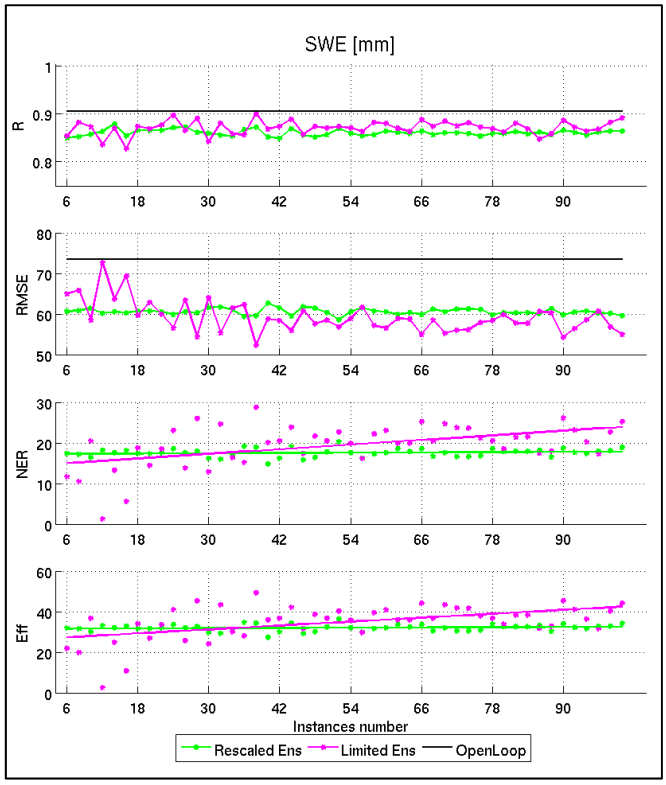

Fig. 11. Comparison between rescaling and truncation of the perturbed ensemble. Variable ensemble size for: a) snow depth, b) snow temperature, c) SWE.

thanks to the slower dynamics of snow depth changes with respect to the thermal ones. Temperature simulation considerably worsens due to the reduction of assimilation frequency, with statistical indices almost equivalent to the open loop ones with a 24-hours assimilation. Conversely, a reduction of the assimilation frequency results in a slight increasing improvement of SWE simulations (Figure 9c). The resulting scores suggest that the useful assimilation frequency for this system lies between 3 and 12 hours.

Exp_s2

The ensemble size is a critical parameter. Indeed, if the amount of model states is too limited, the evaluation of the model error covariance matrix could be not properly accurate. The uncertainty of this estimation decreases in a rate proportional to $1/\sqrt{N}$ with N model states (Evensen, 1994). On the other hand, if the ensemble is oversized, an excessive computational load could be required.

SMASH is not markedly sensitive to the ensemble size, especially in terms of correlation and RMSE. The increasing ensemble size allows an improvement of the assimilation efficiency and NER, whose upward trends are asymptotically tending to an upper limit of model performance (Figure 10).

Figure 11 shows the comparison between two different approaches of limiting the perturbed ensemble in order to guarantee the physical consistency of the system. The green time series refer to the employed method, which consists in rescaling the perturbed ensemble within proper physical limits; magenta ones represent the truncation of the inconsistent values. With respect to the open loop simulations, this latter approach allows an improvement of the snow depth modeling (Figure 11a), but the recurring discarding of inconsistent values does not allow significantly enhancing the surface temperature simulations (Figure 11b). Filter updating of SWE simulation is less sensitive to the implemented approach, with resulting almost equivalent performance (Figure 11c).

Exp_s3

This experiment aims at assessing the efficiency of the multivariable DA scheme depending on the assimilated variables.

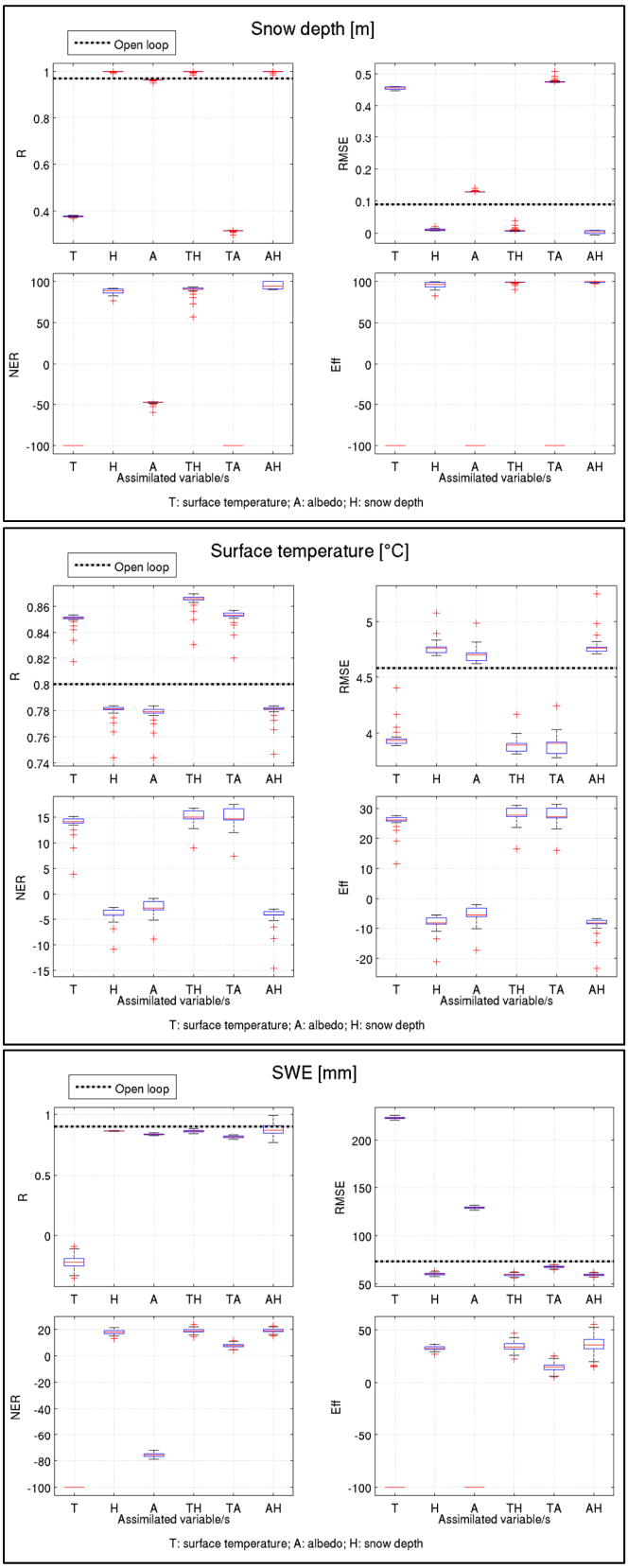

Fig. 12. Exp_s3 – Impact on model performance of the assimilation of different combinations of observed variables for a) snow depth, b) snow temperature, c) SWE.

Figure 12 shows the impact of the assimilation of different combinations of observations. The assimilation of only snow depth observations has a strong impact on snow depth and SWE also when they are assimilated in combination with other observed variables. However, the assimilation of snow depths does not succeed in improving snowpack temperature, even when assimilated together with the surface albedo. The assimilation of only surface temperature measurements has a negative effect on snowpack mass but it guarantees an expected improvement of the modeled temperature, which is even larger through its combined assimilation with snow depth or albedo measurements. The assimilation of only albedo observations has a lower impact on model performance with respect to the control run.

DISCUSSION

The combined assimilation of several ground-based observations allows improving model performance. The multivariable DA has a strong impact on snow depth simulations, both during the accumulation and the melting period. The assimilation of snow depth measurements enables to limit snowpack lowering due to the overestimation of snow compaction during the accumulation season. Moreover, snow melt events during winter and the snowmelt timing are better modeled with respect to the open loop predictions. The filter well succeeds in consistently updating the SWE through a proper handling of model nonlinearities. Indeed, even though no direct measurement of SWE is assimilated, the multivariable EnKF-based DA scheme allows improving SWE model predictions. The assimilation of surface temperature measurements ensures to catch the diurnal and nocturnal peaks, whose values are respectively under- and overestimated by the snow model. Nevertheless, the update of surface temperature introduces a saw tooth pattern in correspondence of the measures assimilation, mainly due to a low model thermal inertia driving the modeled series quickly tend towards the open loop values after the assimilation. Furthermore, it is important to consider that a sharp correction of the surface temperature is likely to generate a thermal condition remarkably different from the current one simulated by the model, which tends to restore its energy balance. The combined assimilation of ground-based measurements and the remote sensed LST entails a worsening of temperature simulations due to the overestimation bias affecting the satellite data. A weaker correction of the surface temperature entails a strengthening in both snow depth and SWE updating. Indeed, the assimilation of snow depth observations is even more effective since snowpack state is less affected by the combined temperature update, which can lead to a resulting thermal condition sensibly different from the modeled one. An expected worsening of the system performance is observed as the assimilation frequency decreases, except for SWE simulation benefiting from a less frequent updating of the energy balance affecting the snow mass. Nevertheless, the multivariable assimilation still allows a significant improvement of model simulations up to every 12 hours. SMASH reveals a low sensitivity to the ensemble size, mainly in terms of RMSE and correlation coefficient. It is important to consider that the larger is the ensemble, the more precise is the evaluation of model error covariance matrix. Anyway, consistently with the results of Durand and Margulis (2006), a sizeable increase of the ensemble (up to 100 model states) does not allow any remarkable improvement. Thus, we can assume that a limited ensemble is likely to provide a reliable assessment. Indeed, the need to enhance the quality of model error has to be balanced by considering the required computational cost.

The rescaling method adopted to constrain the ensemble after its correction and perturbation allows not compromising Gaussian distributions and it results in better performance than the truncation of inconsistent values (Su et al. 2010). Indeed,

the truncation of inconsistent values revealed poorer performance, since it does not preserve the ensemble mean and compromises the perturbations Gaussianity with a resulting bias due to the not null mean-valued perturbations.

The sensitivity analysis of the system to the assimilation of different observed variables allows highlighting the potentials of the multivariable DA scheme. The update of only the energy balance can generate a thermal condition sensibly different from the current one with a resulting worsening of the modeled snow mass. Since the simulated surface temperature is markedly biased, especially at diurnal and nocturnal peaks, its sharp update is likely to strongly impact on the snow depth. For instance, the correction of diurnal temperature peaks can cause snow melting events. On the other hand, the update of only the mass balance has no remarkable impact on the thermal state of the system. Clearly, the reduction of the model error covariance matrix to the energy- and mass-related minors does not guarantee the update of the overall system when individually assimilating energy- or mass-related variables. Nevertheless, the update of any observed variable strongly impacts on the snowpack state. In agreement with Durand and Margulis (2006) demonstrating the benefit of jointly assimilating energy- and mass-related observations, the resulting largest overall enhancement of model state is guaranteed by the combined assimilation of surface temperature, snow depth measurements and albedo.

CONCLUSION AND FUTURE DEVELOPMENTS

This research aims at investigating the feasibility of assimilating several ground-based snow observations for real-time applications by implementing new approaches allowing to better handle several limiting issues (e.g. model nonlinearities; computational demand). The main focus of the study is the assessment of the impact of different settings of the DA system on the performance of the multivariable EnKF. SMASH consists in a multi-layer model able to reproduce some of the main physical processes affecting snowpack dynamics by solving both energy and mass balances. An EnKF scheme is used to jointly assimilate observations of several variables of interest. Several constraints are introduced to maintain the model physical coherence. The model error covariance matrix is reduced to energy- and mass-related minors in order to prevent the introduction of any spurious correction of indirect state variables resulting from the nonlinear correlations among them. Moreover, any inconsistent value of the state variables resulting from the analysis procedure and/or the perturbation of the ensemble states is removed by limiting each variable into a proper physical range. Since the system is supposed to solve the energy balance both in snowy and snowless conditions, time variant physical ranges are modulated according to both air temperature and snow mass in order to properly handling transition periods (early winter and melting season) without causing model instability. SMASH 1D-version was tested at Torgnon site throughout the period June 2012 – December 2013. Several ground-based measurements were assimilated every 3 hours: surface temperature, snow depth and albedo. Data assimilation succeeds in enhancing model performance by reducing snow model biases in terms of surface temperature, SWE and snow depth. As well, the joint assimilation of ground-based measurements (snow depth and albedo) and remote sensed LST from MSG allowed improving model predictions, even though the large overestimation bias of the satellite observations compromises temperature simulations. Several sensitivity experiments were performed to assess SMASH sensitivity to different assimilation settings. With the decreasing of the assimilation frequency from 3 to 24 hours, the system revealed an expected worsening of modeling performance, except for SWE simulations. A 12-hours DA still guarantees significant improvements of model simulations. The lack of remarkable improvements with an increasing amount of model states reveals that SMASH is not markedly sensitive to the ensemble size. From a computational point of view, it is a considerable benefit since it enables to achieve well-performing results even employing a limited ensemble. The evaluation of the system sensitivity to the assimilation of different combinations of observed variables gives evidence of the potentialities of the multivariable DA. Indeed, the combined assimilation of surface temperature, snow depth and albedo observations reveals the best results in snowpack modeling. In light of the promising performance of the multivariable EnKF achieved in this point application, the development of the distributed version of the system is planned. The spatialized DA scheme is intended to enable a multisensory assimilation of several satellite products (e.g. MODIS SCA and snow albedo; Meteosat surface temperature; LiDAR measurements of snow depth; SWE from passive microwave sensors) for hydrological applications.

REFERENCES

Anderson, E.A, 1976. A point of energy and mass balance model of snow cover. NOAA Tech. Rep. NWS, 19, 150 p.

Andreadis, K.M., Lettenmaier, D.P., 2005. Assimilating remotely sensed snow observations into a macroscale hydrology model. Advances in Water Resources, 29.6, 872–886.

Avanzi, F., De Michele, C., Morin, S., Carmagnola, C.M., Ghezzi, A., Lejeune, Y., 2016. Model complexity and data requirements in snow hydrology: seeking a balance in practical applications. Hydrol. Process., 30, 2106–2118.

Balsamo, G., Albergel, C., Beljaars, A., Boussetta, S., Brun, E., Cloke, H., Dee, D., Dutra, E., Muñoz-Sabater, J., Pappenberger, F., de Rosnay, P., Stockdale, T., Vitart, F., 2015. ERA-Interim/Land: a global land surface reanalysis data set. Hydrology and Earth System Sciences, 19, 1, 389–407.

Barnett, T.P., Adam, J.C., Lettenmaier, D.P., 2005. Potential impacts of a warming climate on water availability in snow-dominated regions. Nature, 438, 7066, 303–309.

Bartelt, P., Lehning, M., 2002. A physical SNOWPACK model for the Swiss avalanche warning: Part I: numerical model. Cold Regions Science and Technology, 35, 3, 123–145.

Boni, G., Castelli, F., Gabellani, S., Machiavello, G., Rudari, R., 2010. Assimilation of MODIS snow cover and real time snow depth point data in a snow dynamic model. In: Proc. Geoscience and Remote Sensing Symposium (IGARSS). IEEE International, pp. 1788–1791.

Boone, A., Etchevers, P., 2001. An intercomparison of three snow schemes of varying complexity coupled to the same land surface model: Local-scale evaluation at an Alpine site. Journal of Hydrometeorology, 2, 4, 374–394.

Boone, A., Habets, F., Noilhan, J., Clark, D., Dirmeyer, P., Fox, S., Gusev, Y., Haddeland, I., Koster, R., Lohmann, D., Mahanama, S., Mitchell, K., Nasonova, O., Niu, G.-Y., Pitman, A., Polcher,J., Shmakin, A. B., Tanaka, K., van den Hurk, B., Vérant, S., Verseghy, D., Viterbo, P., Yang, Z.-L., 2004. The Rhone-aggregation land surface scheme intercomparison project: An overview. Journal of Climate, 17, 1, 187–208.

Bowling, L.C., Lettenmaier, D.P., Nijssen, B., Graham, L.P., Clark, D.B., El Maayar, M., Essery, R., Goers, S., Gusev, Y.M., Habets, F., van den Hurk, B., Jin, J., Kahan, D., Lohmann, D., Ma, X., Mahanama, S., Mocko, D., Nasonova,

O., Niu, G., Samuelsson, P., Shmakin, A.B., Takata, K., Verseghy, D., Viterbo, P., Xia, Y., Xue, Y., Tang, Z., 2003. Simulation of high-latitude hydrological processes in the Torne–Kalix basin: PILPS Phase 2 (e): 1: Experiment description and summary intercomparisons. Global and Planetary Change, 38, 1, 1–30.

Brasnett, B., 1999. A global analysis of snow depth for numerical weather prediction. Journal of Applied Meteorology, 38, 6, 726–740.

Brocca, L., Moramarco, T., Melone, F., Wagner, W., Hasenauer, S., Hahn, S., 2012. Assimilation of surface-and root-zone ASCAT soil moisture products into rainfall–runoff modeling. IEEE Transactions on Geoscience and Remote Sensing, 50, 7, 2542–2555.

Brun, E., Martin, E., Simon, V., Gendre, C., Coleou, C., 1989. An energy and mass model of snow cover suitable for operational avalanche forecasting. Journal of Glaciology, 35, 121, 333–342.

Caparrini, F., Castelli, F., Entekhabi, D., 2004. Estimation of surface turbulent fluxes through assimilation of radiometric surface temperature sequences. Journal of Hydrometeorology, 5, 1, 145–159.

Charrois, L., Cosme, E., Dumont, M., Lafaysse, M., Morin, S., Libois, Q., Picard, G., 2016. On the assimilation of optical reflectances and snow depth observations into a detailed snowpack model. The Cryosphere, 10, 1021–1038. http://doi.org/10.5194/tc-10-1021-2016.

Chen, F., Crow, W.T., Starks, P.J., Moriasi, D.N., 2011. Improving hydrologic predictions of a catchment model via assimilation of surface soil moisture. Advances in Water Resources, 34, 4, 526–536.

Clark, M.P., Hay, L.E., 2004. Use of medium-range numerical weather prediction model output to produce forecasts of stream-flow. J. Hydrometeorol., 5, 15–32.

Clark, M.P., Slater, A.G., Barrett, A.P., Hay, L.E., McCabe, G.J., Rajagopalan, B., Leavesley, G.H., 2006. Assimilation of snow covered area information into hydrologic and land-surface models. Advances in Water Resources, 29, 8, 1209–1221.

Cressman, G.P., 1959. An operational objective analysis system. Mon. Wea. Rev., 87, 10, 367–374.

Dee, D.P., Uppala, S.M., Simmons, A.J., Berrisford, P., Poli, P., Kobayashi, S., Andrae, U., Balmaseda, M.A., Balsamo, G., Bauer, P., Bechtold, P., Beljaars, A.C.M., van de Berg, L. Bidlot, J., Bormann, N., Delsol, C., Dragani, R., Fuentes, M., Geer, A.J., Haimberger, L., Healy, S.B., Hersbach, H., Hòlm, E.V., Isaksen, L., Kållberg, P., Köhler, M., Matricardi, M., McNally, A.P., Monge-Sanz, B.M., Morcrette, J.-J. , Park, B.-K., Peubey, C., deRosnay, P., Tavolato, C., Thépaut, J.-N., Vitart, F., 2011. The ERA-Interim reanalysis: Configuration and performance of the data assimilation system. Quarterly Journal of the Royal Meteorological Society, 137, 656, 553–597.

De Lannoy, G.J.M., Reichle, R.H., Arsenault, K.R., Houser, P.R., Kumar, S., Verhoest, N.E.C., Pauwels, V.R.N., 2012. Multiscale assimilation of advanced microwave scanning radiometer-EOS snow water equivalent and moderate resolution imaging spectroradiometer snow cover fraction observations in northern Colorado. Water Resour. Res., 48, W01522. DOI: 10.1029/2011WR010588.

Dong, J., Walker, J.P., Houser, P.R., Sun, C., 2007. Scanning multichannel microwave radiometer snow water equivalent assimilation. Journal of Geophysical Research: Atmospheres, 112, D7.

Douville, H., Royer, J.-F., Mahfouf, J.-F., 1995. A new snow parameterization for the Meteo-France climate model Part I: validation in stand-alone experiments. Climate Dynamics, 12, 1, 21–35.

Drusch, M., Vasiljevic, D., Viterbo, P., 2004. ECMWF's global snow analysis: assessment and revision based on satellite observations. J. Appl. Meteorol., 43, 1282–1294.

Dunne, S., Entekhabi, D., 2005. An ensemble-based reanalysis approach to land data assimilation. Water Resour. Res., 41, 2.

Dunne, S., Entekhabi, D., 2006. Land surface state and flux estimation using the ensemble Kalman smoother during the Southern Great Plains 1997 field experiment. Water Resour. Res., 42, 1.

Durand, M., Margulis, S.A., 2006. Feasibility test of multifrequency radiometric data assimilation to estimate snow water equivalent. Journal of Hydrometeorology, 7, 3, 443–457.

Durand, M., Margulis, S.A., 2008. Effects of uncertainty magnitude and accuracy on assimilation of multiscale measurements for snowpack characterization. J. Geophys. Res. Atmos., 113, D02105.

Dutra, E., Balsamo, G., Viterbo, P., Miranda, P.M., Beljaars, A., Schär, C., Elder, K., 2010. An improved snow scheme for the ECMWF land surface model: description and offline validation. Journal of Hydrometeorology, 11, 4, 899–916.

Dutra, E., Viterbo, P., Miranda, P.M., Balsamo, G., 2012. Complexity of snow schemes in a climate model and its impact on surface energy and hydrology. Journal of Hydrometeorology, 13, 2, 521–538.

Endrizzi, S., Gruber, S., Dall'Amico, M., Rigon, R., 2014. GEOtop 2.0: simulating the combined energy and water balance at and below the land surface accounting for soil freezing, snow cover and terrain effects. Geoscientific Model Development, 7, 2831–2857.

Essery, R., Rutter, N., Pomeroy, J., Baxter, R., Stahli, M., Gustafsson, D., Barr, A., Bartlett, P., Elder, K., 2009. SNPWMIP2: An evaluation of forest snow process simulations. Bull. Amer. Met. Soc., 90, 1120–1135.

Essery, R., Morin, S., Lejeune, Y., Ménard, C.B., 2013. A comparison of 1701 snow models using observations from an Alpine site. Advances in Water Resources, 55, 131–148.

Etchevers, P., Martin, E., Brown, R., Fierz, C., Lejeune, Y., Bazile, E., Boone, A., Dai, Y.J., Essery, R., Fernandez, A., Gusev, Y., Jordan, R., Koren, V., Kowalczyk, E., Nasonova, N.O., Pyles, R.D., Schlosser, A., Shmakin, A.B., Smirnova, T.G., Strasser, U., Verseghy, D., Yamazaki, T., Yang, Z.L., 2003. Validation of the energy budget of an alpine snowpack simulated by several snow models (SnowMIP project). Annals of Glaciology, 38, 1, 150–158.

Evensen, G., 1994. Sequential data assimilation with a nonlinear quasi-geostrophic model using Monte Carlo methods to forecast error statistics. Journal of Geophysical Research: Oceans, 99, C5, 10143–10162.

Evensen, G., 2003. The ensemble Kalman filter: Theoretical formulation and practical implementation. Ocean Dynamics, 53, 4, 343–367.

Filippa, G., Cremonese, E., Galvagno, M., Migliavacca, M., Di Cella, U.M., Petey, M., Siniscalco, C., 2015. Five years of phenological monitoring in a mountain grassland: inter-annual patterns and evaluation of the sampling protocol. International journal of biometeorology, 59, 12, 1927–1937.

Froidurot, S., Zin, I., Hingray, B., Gautheron, A., 2014. Sensitivity of precipitation phase over the Swiss Alps to different meteorological variables. Journal of Hydrometeorology, 15, 2, 685–696.

Galvagno, M., Wohlfahrt, G., Cremonese, E., Rossini, M., Colombo, R., Filippa, G., Julitta, T., Manca, G., Siniscalco, C., Migliavacca, M., Morra di Cella, U., 2013. Phenology and carbon dioxide source/sink strength of a subalpine grassland in response to an exceptionally short snow season. Environmental Research Letters, 8, 2, 025008.

Gelb, A., 1974. Optimal linear filtering, in Applied Optimal Estimation, edited by A. Gelb, pp. 102–155, MIT Press, Cambridge, Mass.

Griessinger, N., Seibert, J., Magnusson, J., Jonas, T., 2016. Assessing the benefit of snow data assimilation for runoff modeling in Alpine catchments. Hydrology and Earth System Sciences, 20, 9, 3895–3905.

Gupta, H.V., Kling, H., Yilmaz, K.K., Martinez, G.F., 2009. Decomposition of the mean squared error and NSE performance criteria: Implications for improving hydrological modelling. Journal of Hydrology, 377, 1, 80–91.

Hedstrom, N.R., Pomeroy, J.W., 1998. Accumulation of intercepted snow in the boreal forest: measurements and modelling. Hydrological Processes, 12, 1611–1625.

Huang, C., Newman, A.J., Clark, M.P., Wood, A.W., Zheng, X., 2017. Evaluation of snow data assimilation using the ensemble Kalman filter for seasonal streamflow prediction in the western United States. Hydrology and Earth System Sciences, 21 1, 635–650.

Jordan, R., 1991. A one-dimensional temperature model for a snow cover: Technical documentation for SNTHERM. 89 (No. CRREL-SR-91-16). Cold Regions Research and Engineering Lab Hanover, NH.

Jimenez-Munoz, J.C., Sobrino, J.A., 2008. Split-window coefficients for land surface temperature retrieval from low-resolution thermal infrared sensors. IEEE geoscience and remote sensing letters, 5, 4, 806–809.

Kojima, K., 1967. Densification of a seasonal snow cover, in Physics of Snow and Ice, Proc. Int. Conf. Low Temp. Sci., vol. I, part 2, S.929-S.952.

Lehning M., Bartelt, P.B., Brown, R.L., Fierz, C., Satyawali, P., 2002. A physical SNOWPACK model for the Swiss Avalanche Warning Services. Part II: Snow Microstructure. Cold regions science and technology, 35, 3, 147–167.

Liston, G.E., Sturm, M., 1998. A snow-transport model for complex terrain. Journal of Glaciology, 44, 148, 498–516.

Liston, G.E., Pielke, R.A., Greene, E.M., 1999. Improving first-order snow-related deficiencies in a regional climate model. Journal of Geophysical Research: Atmospheres, 104(D16), 19559–19567.

Liston, G.E., Hiemstra, C.A., 2008. A simple data assimilation system for complex snow distributions (SnowAssim). Journal of Hydrometeorology, 9, 5, 989–1004.

Magnusson, J., Farinotti, D., Jonas, T., and Bavay, M., 2011. Quantitative evaluation of different hydrological modelling approaches in a partly glacierized Swiss watershed. Hydrol. Process., 25, 2071–2084.

Magnusson, J., Gustafsson, D., Hüsler, F., Jonas, T., 2014. Assimilation of point SWE data into a distributed snow cover model comparing two contrasting methods. Water Resources Research, 50, 10, 7816–7835.

Magnusson, J., Wever, N., Essery, R., Helbig, N., Winstral, A., Jonas, T., 2015. Evaluating snow models with varying process representations for hydrological applications: Snow model evaluation. Water Resour. Res., 51, 2707–2723.

Malik, M.J., van der Velde, R., Vekerdy, Z., Su, Z., 2012. Assimilation of satellite-observed snow albedo in a land surface model. Journal of hydrometeorology, 13, 3, 1119–1130.

Mellor, M., 1964. Properties of snow, Cold Reg. Sci. Eng. Monogr., III-A1.

Miller, R.N., Ghil, M., Gauthiez, F., 1994. Advanced data assimilation in strongly nonlinear dynamical systems. Journal of the atmospheric sciences, 51, 8, 1037–1056.

Montzka, C., Pauwels, V., Franssen, H.J.H., Han, X., Vereecken, H., 2012. Multivariate and multiscale data assimilation in terrestrial systems: A review. Sensors, 12, 12, 16291–16333.

Moradkhani, H., 2008. Hydrologic remote sensing and land surface data assimilation. Sensors, 8, 5, 2986–3004.

Nijssen, B., Bowling, L.C., Lettenmaier, D.P., Clark, D.B., El Maayar, M., Essery, R.,Goers, S., Gusev, Y.M., Habets, F., van den Hurk, B., Jin, J., Kahan, D., Lohmann, D., Ma, X., Mahanama, S., Mocko, D., Nasonova, O., Niu, G., Samuelsson, P., Shmakin, A.B., Takata, K., Verseghy, D., Viterbo, P., Xia, Y., Xue, Y., Yang, Z., 2003. Simulation of high latitude hydrological processes in the Torne–Kalix basin: PILPS Phase 2 (e): 2: Comparison of model results with observations. Global and Planetary Change, 38, 1, 31–53.

Pan, M., Sheffield, J., Wood, E.F., Mitchell, K.E., Houser, P.R., Schaake, J.C., Robock, A., Lohmann, D., Cosgrove, B., Duan, Q., Luo, L., Higgins, R.W., Pinker, R.T., Tarpley, J.D., 2003. Snow process modeling in the North American Land Data Assimilation System (NLDAS): 2. Evaluation of model simulated snow water equivalent. Journal of Geophysical Research: Atmospheres, 108, D22.

Rodell, M., Houser, P.R., 2004. Updating a land surface model with MODIS-derived snow cover. Journal of Hydrometeorology, 5, 6, 1064–1075.

Rutter, N., Essery, R., Pomeroy, J., Altimir, N., Andreadis, K., Baker, I., Barr, A., Bartlett, P., Boone, A., Deng, H., Douville, H., Dutra, E., Elder, K., Ellis, C., Feng, X., Gelfan, A., Goodbody, A., Gusev, Y., Gustafsson, D., Hellström, R., Hirabayashi, Y., Hirota, T., Jonas, T., Koren, V., Kuragina, A., Lettenmaier, D., Li, W.-P., Luce, C., Martin, E., Nasonova, O., Pumpanen, J., Pyles, R.D., Samuelsson, P., Sandells, M., Schädler, G., Shmakin, A., Smirnova, T.G., 27, Stähli, M., Stöckli, R., Strasser, U., Su, H., Suzuki, K., Takata, K., Tanaka, K., Thompson, E., Vesala, T., Viterbo, P., Wiltshire, A., Xia, K., Xue, Y., Yamazaki, T., 2009. Evaluation of forest snow processes models (SnowMIP2). Journal of Geophysical Research: Atmospheres, 114, D6.

Schlosser, C.A., Slater, A.G., Robock, A., Pitman, A.J., Vinnikov, K.Y., Henderson-Sellers, A., Speranskaya, N.A., Mitchell, K., and the PILPS2 contributors, 2000. Simulations of a boreal grassland hydrology at Valdai, Russia: PILPS Phase 2 (d). Monthly Weather Review, 128, 2, 301–321.

Slater, A.G., Pitman, A.J., Desborough, C.E., 1998. The validation of a snow parameterization designed for use in general circulation models. International journal of climatology, 18, 6, 595–617.

Slater, A.G., Schlosser, C.A., Desborough, C.E., Pitman, A.J., Henderson-Sellers, A., Robock, A., Vinnikov, K.Y., Mitchell, K., Boone, A., Braden, H., Chen, F., Cox, P.M., de Rosnay, P., Dickinson, R.E., Dai,Y.-J., Duan ,Q., Entin, J., Etchevers, P., Gedney, N., Gusev, Y.M., Habets, F., Kim, J., Koren, V., Kowalczyk, E.A., Nasonova, O.N., Noilhan, J., Schaake, S., Shmakin, A.B., Smirnova, T.G., Verseghy, D., Wetzel, P., Xue, Y., Yang, Z.-L., Zeng, Q., 2001. The representation of snow in land surface schemes: Results from PILPS 2 (d). Journal of Hydrometeorology, 2, 1, 7–25.

Slater, A.G., Clark, M.P., 2006. Snow data assimilation via an ensemble Kalman filter. Journal of Hydrometeorology, 7, 3, 478–493.

Stauffer, D.R., Seaman, N.L., 1990. Use of four-dimensional data assimilation in a limited-area mesoscale model. Part I: Experiments with synoptic-scale data. Monthly Weather Review, 118, 6, 1250–1277.

Stigter, E.E., Wanders, N., Saloranta, T.M., Shea, J.M., Bierkens, M.F.P., Immerzeel, W.W., 2017. Assimilation of snow cover and snow depth into a snow model to estimate snow water equivalent and snowmelt runoff in a Himalayan catchment, Cryosph., 1647–1664.

Su, H., Yang, Z.L., Niu, G.Y., Dickinson, R.E., 2008. Enhancing the estimation of continental-scale snow water equivalent by assimilating MODIS snow cover with the ensemble Kalman filter. Journal of Geophysical Research: Atmospheres, 113, D8.

Su, H., Yang, Z.L., Dickinson, R.E., Wilson, C.R., Niu, G.Y., 2010. Multisensor snow data assimilation at the continental scale: The value of gravity recovery and climate experiment terrestrial water storage information. Journal of Geophysical Research: Atmospheres, 115, D10.

Sun, C., Walker, J.P., Houser, P.R., 2004. A methodology for snow data assimilation in a land surface model. Journal of Geophysical Research: Atmospheres, 109, D8.

Verseghy, D.L., 1991. CLASS–A Canadian land surface scheme for GCMs. I. Soil model. International Journal of Climatology, 11, 2, 111–133.

Vionnet, V., Brun, E., Morin, S., Boone, A., Faroux, S., Le Moigne, P., Martin, E., Willemet, J.M., 2012. The detailed snowpack scheme Crocus and its implementation in SURFEX v7. 2. Geoscientific Model Development, 5, 773–791.

Wächter, A., Biegler, L.T., 2006. On the implementation of an interior-point filter line-search algorithm for large-scale nonlinear programming. Mathematical Programming, 106, 1, 25–57.

Winstral, A., Marks, D., 2014. Long-term snow distribution observations in a mountain catchment: Assessing variability, time stability, and the representativeness of an index site. Water Resources Research, 50, 1, 293–305.

Wiscombe, W.J., Warren, S.G., 1980. A model for the spectral albedo of snow. I: Pure snow. Journal of the Atmospheric Sciences, 37, 12, 2712–2733.

Wood, A.W., Hopson, T., Newman, A., Brekke, L., Arnold, J., Clark, M., 2016. Quantifying streamflow forecast skill elasticity to initial condition and climate prediction skill. Journal of Hydrometeorology, 17, 2, 651–668.

Zappa, M., Pos, F., Strasser, U., Warmerdam, P., Gurtz, J., 2003. Seasonal water balance of an Alpine catchment as evaluated by different methods for spatially distributed snowmelt modelling. Hydrology Research, 34, 3, 179–202.

Zhang, T., 2005. Influence of the seasonal snow cover on the ground thermal regime: An overview. Reviews of Geophysics, 43, 4.

Yang, Z.L., Dickinson, R.E., Robock, A., Vinnikov, K.Y., 1997. Validation of the snow submodel of the biosphere–atmosphere transfer scheme with Russian snow cover and meteorological observational data. Journal of Climate, 10, 2, 353–373.

Received 18 May 2017
Accepted 11 December 2017